Center for Management Science Research
ISSN: 3006-5291 3006-5283 Volume 3, Issue 3, 2025

AN EFFICIENT HYBRID B-SPLINE APPROACH FOR NUMERICAL APPROXIMATION OF TIME-FRACTIONAL TELEGRAPH EQUATIONS

Muhammad Waqas[*1], Muhammad Amin[2], Saima Mushtaq[3]

[*1,2,3]*Faculty of Sciences, The Superior University Lahore, Pakistan.*

[*1]muhammadwaqas494@gmail.com

DOI: https://doi.org/10.5281/zenodo.15744369

Keywords
Time fractional telegraph equation; Caputo fractional derivative; Finite difference Formulae; Cubic B Spline; Hybrid Cubic B Spline; Convergence

Article History
Received on 18 May 2025
Accepted on 18 June 2025
Published on 26 June 2025

Corresponding Author: * Muhammad Waqas

Abstract
Telegraph equations are hyperbolic partial differential equations that display diffusion reaction processes in a biological and engineering field. The main purpose of this work is to solve time fractional telegraph equation using spline functions especially the application of Hybrid cubic B-spline (HCBS) functions. The proposed method utilizes HCBS functions to interpolate the solution curve over the spatial grid, while the time fractional derivative is discretized using the Caputo fractional derivative formula. The basic objective of the study is to developed a numerical solution for an initial boundary value issue by using finite difference methods for a hyperbolic equation. Accordingly, this study introduces a method based on finite difference formulas and time-frequency analysis to address initial boundary value problems. The stability and convergence of the approach are established through conventional analytical methods, confirming that the scheme is unconditionally stable and exhibits a specific convergence rate. To validate the theoretical results, various numerical experiments are carried out. Additionally, the plotted results demonstrate a strong correlation between the exact and computed solutions, highlighting the precision of the technique.

INTRODUCTION
In recent years, Fractional Differential Equations (FDEs) have attracted considerable attention from scientists and engineers worldwide due to their wide range of applications in areas such as quantum mechanics, astrophysics, signal processing, engineering, classical mechanics, hydrology, electrochemistry, hadron spectroscopy, probability theory, heat conduction, and diffusion-related problems [1,3]. Over the past two decades, the fractional telegraph equation has been extensively investigated by numerous researchers [2,7]. This equation serves as a fundamental mathematical model for analyzing wave propagation and electrical signal transmission in conductors. It belongs to the class of hyperbolic partial differential equations [5]. Benson first highlighted the significance of the Fractional Telegraph Equation (FTE) in 2001, exploring its various characteristics in the context of time-fractional dynamics [15]. Further studies, including [10,17], have applied techniques such as the Adomian Decomposition Method to solve both time- and space-fractional forms of the telegraph equation. Dehghan et al. [25] addressed the solution of multi-dimensional space telegraph equations using the projected variational method. To derive analytical solutions for telegraph equations with fractional time derivatives, researchers in [23,25] utilized the homotopy analysis method. Subsequently, Hayat et al. [27] employed the homotopy perturbation method to investigate time-fractional telegraph equations, considering both Brownian and standard motion scenarios. Nasrin

Samadyar [6,10] proposed a solution technique for the two-dimensional time fractional stochastic Tricomi type equation by applying the Caputo derivative in the temporal direction, coupled with Neumann boundary conditions. This method operates within an irregular domain using a meshless approach grounded in the finite difference framework. In a related effort, Farshid Mirzaee [6,10] applied the quintic B-spline collocation method to numerically solve stochastic Itô–Volterra integral equations. H. Hassani [7] introduced the transcendental Bernstein series (TBS), a generalization of classical Bernstein polynomials, to solve variable-order space-time fractional telegraph equations (V-STFTE). Wang [14] investigated the use of the mixed finite element method for a nonlinear time-fractional wave model to address numerical solutions of the time-fractional telegraph equation (TFTE). For other numerical techniques, Modanli et al. [21] implemented the Theta method to approximate the solution of the fractional-order telegraph equation, while Xu et al. [23] applied the Legendre wavelet-based direct approach. In works [22,27], Wang and colleagues employed the spectral Galerkin method to obtain approximate solutions for the TFTE. Kamran et al. [8,31,34,36] developed a localized kernel-based method for the numerical treatment of the TFTE. Muhammad Yaseen [11] proposed a technique involving cubic trigonometric B-splines for spatial derivatives and finite difference schemes for the Caputo time-fractional derivative to solve TFTE numerically. Modanli [32] explored fractional-order operators, particularly the Atangana–Baleanu model, in modeling the spread of COVID-19. Akram and Tariq devised a quintic spline collocation approach to handle fractional boundary value problems, while cubic B-spline collocation techniques were applied to fractional diffusion problems. Additionally, a quintic B-spline collocation scheme was used to solve a fourth-order time-fractional super-diffusion equation. The TFTE has also been tackled using the quadratic B-spline Galerkin method, as demonstrated by M. Shivhare in 2021 [13].

In this study, the time-fractional telegraph equation is considered in its most general mathematical form as follows:

$$\frac{\partial^{\beta}}{\partial t^{\beta}}u(s,t)+\frac{\partial^{\gamma}}{\partial t^{\gamma}}u(s,t)+\alpha_1 u(s,t)-\alpha_2\frac{\partial^2}{\partial s^2}u(s,t)=f(s,t),$$

$$(s,t)\in(0,L)\times(0,T) \qquad (A)$$

$$u(s,0)=\phi_1(s),\quad u_t(s,0)=\phi_2(s), s\in[0,L] \qquad (B)$$

$$u(0,t)=\psi_1(t),\quad u(L,t)=\psi_2(t), t\in[0,T] \qquad (C)$$

where Caputo fractional derivatives of order β and γ respectively are represented by $\frac{\partial^{\beta}}{\partial t^{\beta}}u(s,t), \frac{\partial^{\gamma}}{\partial t^{\gamma}}u(s,t)$ and $\phi_j(s)$ and $\psi_j(t)(j=1,2)$ are given. In eq (A), $\beta\in(1,2]$ and $\gamma\in(0,1]$. However, this study is limited to the class of problems relating $\beta=\gamma+1$ and $\beta=2\gamma$.

In this study, a Hybrid Cubic B-Spline (HCBS) approach is employed to obtain the numerical solution of the time-fractional telegraph equation (TFTE). The HCBS functions, characterized by a single shape-controlling parameter, represent a generalized form of classical cubic B-splines, offering enhanced flexibility in shaping the solution curve [30]. Despite this generalization, the continuity of the HCBS functions remains at order three, while the degree of the piecewise polynomial segments is increased by one. The Caputo time-fractional derivative is discretized using a finite difference scheme. In conventional collocation methods, Dirichlet boundary conditions are often applied where the spline basis functions typically vanish. However, standard HCBS functions do not naturally vanish at the boundaries. To address this, a tailored form of HCBS functions is used for spatial discretization, ensuring that they satisfy Dirichlet-type conditions by vanishing at the domain boundaries. To the best of our knowledge, this novel strategy has not been previously applied to approximate solutions of fractional partial differential equations (PDEs).

The structure of this manuscript is as follows: Section 2 introduces the definition of Hybrid Cubic B-Spline functions. Section 3 describes the proposed numerical scheme. Section 4 presents the stability analysis of the method. Section 5 provides a theoretical convergence analysis. Section 6 discusses the numerical results and their interpretation. Section 7 concludes the paper with final remarks.

1. Hybrid Cubic B-Spline Functions

Let the spatial domain$[a,b]$ is divided into M subintervals of length $h=\frac{b-a}{M}$, such that the grid points are defined by $a=s_0<s_1<\cdots<s_M=b$, where $s_m=s_0+mh, \text{for } m=0,1\ldots\ldots\ldots,M$. To approximate a sufficiently smooth function $U^*(s,t)$ we consider the HCBS-based approximation $u(s,t)$ is given by

$$U^*(s,t)=\sum_{m=-1}^{M+1}\varpi_m(t)\kappa_m(s,\lambda) \qquad (1.1)$$

where $\varpi_m(t)$ are time-dependent coefficients (real-valued functions), and $\kappa_m(s,\lambda)$ denote the Hybrid Cubic B-Spline (HCBS) basis functions parameterized by λ [40]:

$$\kappa_m(s,\lambda)=\frac{1}{24h^4}\begin{cases}4(1-\lambda)h(s-s_{m-2})^3+3\lambda(s-s_{m-2})^4, & \text{if } s\in[s_{m-2},s_{m-1})\\ (4-\lambda)h^4+12h^3(s-s_{m-1})+6h^2+(2+\lambda)(s-s_{m-1})^2 & \\ -12h(s-s_{m-1})^3-3\lambda(s-s_{m-1})^4, & \text{if } s\in[s_{m-1},s_m)\\ (4-\lambda)h^4-12h^3(s-s_{m+1})-6h^2(2+\lambda)(s-s_{m+1})^2 & \\ +12h(s-s_{m+1})^3+3\lambda(s-s_{m-1})^4, & \text{if } s\in[s_m,s_{m+1})\\ -4h(1-\lambda)(s-s_{m+2})^3-3\lambda(s-s_{m+2})^4, & \text{if } s\in[s_{m+1},s_{m+2})\\ 0, & \text{otherwise}\end{cases} \qquad (1.2)$$

The parameter λ which lies in the range $-8\le\lambda\le 1$ is introduced to control and fine-tune the shape of the spline curve. The approximate solution at the m[th] spatial node and the r[th] time level is denoted by $(U^*)_m^r=U^*(s_m,t^r)$. Furthermore, the approximate solution and its first and second spatial derivatives with respect to space variable s, in terms of ϖ_m can be expressed as Where the parameter λ range $-8\le\lambda\le 1$ is used to fine tune the shape of the curve. The approximate solution at m[th] spatial node and r[th] time step denoted by $(U^*)_m^r=U^*(s_m,t^r)$ along with its first two derivatives with respect to space variable s, in terms of ϖ_m can be expressed as

$$\begin{cases}(U^*)_m^r=C_1\varpi_{m-1}^r+C_2\varpi_m^r+C_1\varpi_{m+1}^r,\\ (U_s^*)_m^r=-C_3\varpi_{m-1}^r+C_3\varpi_{m+1}^r,\\ (U_{ss}^*)_m^r=C_4\varpi_{m-1}^r+C_5\varpi_m^r+C_4\varpi_{m+1}^r,\end{cases} \qquad (1.3)$$

where $C_1=\frac{4-\lambda}{24}, C_2=\frac{16+2\lambda}{24}, C_3=\frac{1}{2h}, C_4=\frac{2+\lambda}{2h^2}, C_5=\frac{-4-2\lambda}{2h^2}$. The HCBS basis functions $\kappa_{-1},\kappa_0,\ldots,\kappa_{M+1}$ generally do not vanish at the boundaries of the domain, which poses a challenge when applying Dirichlet boundary conditions. To overcome this issue, the basis functions are modified such that the resulting set satisfies the condition of vanishing at the domain endpoints [39]. As a result, the coefficients ϖ_{-1}^r and ϖ_{M+1}^r associated with the boundary-violating basis functions are eliminated from the approximation expression in Eq. (1.1), leading to a reduced form:

$$U(s,t)=\varphi(s,t)+\sum_{m=0}^{M}\varpi_m^r(t)\tilde{\kappa}_m(s,\lambda) \qquad (1.4)$$

where the weight function $\varphi(s,t)$ and HCBS functions are given by

$$\varphi(s,t)=\frac{\kappa_{-1}(s,\lambda)}{\kappa_{-1}(s_0,\lambda)}\psi_1(t)+\frac{\kappa_{M+1}(s,\lambda)}{\kappa_{M+1}(s_M,\lambda)}\psi_2(t) \qquad (1.5),$$

$$\begin{cases}\tilde{\kappa}_m(s,\lambda)=\kappa_m(s,\lambda)-\frac{\kappa_m(s_0,\lambda)}{\kappa_{-1}(s_0,\lambda)}\kappa_{-1}(s,\lambda), & m=0,1\\ \tilde{\kappa}_m(s,\lambda)=\kappa_m(s,\lambda), & m=2{:}1{:}M-2\\ \tilde{\kappa}_m(s,\lambda)=\kappa_m(s,\lambda)-\frac{\kappa_m(s_M,\lambda)}{\kappa_{M+1}(s_M,\lambda)}\kappa_{M+1}(s,\lambda), & m=M-1,M\end{cases} \qquad (1.6)$$

2. Numerical Framework

The Caputo's time fractional derivative of order $\alpha \in (1,2]$ can be discretize at $t = t_{r+1}$. The time interval $[0, T]$ is divided into R subintervals $[t_r, t_{r+1}]$. Where $t_r = r\Delta t, r = 0,1,2, \dots, R$ and $\Delta t = \frac{T}{R}$. at $t = t_{r+1}$.

$$\begin{aligned}
\frac{\partial^\beta}{\partial t^\beta} u(s, t_{r+1}) &= \int_{t_0}^{t_{r+1}} \frac{\partial^2 u(s,w)}{\partial w^2} \frac{(t_{r+1} - w)^{-\beta+1}}{\Gamma(2-\beta)} dw, \\
&= \frac{1}{\Gamma(2-\beta)} \sum_{j=0}^{r} \int_{t_j}^{t_{j+1}} \frac{\partial^2 u(s,w)}{\partial w^2} (t_{r+1} - w)^{-\beta+1} dw, \\
&= \frac{1}{\Gamma(2-\beta)} \sum_{j=0}^{r} \frac{u(s,t_{j+1}) - 2u(s,t_j) + u(s,t_{j-1})}{\Delta t^2} \int_{t_j}^{t_{j+1}} (t_{r+1} - w)^{-\beta+1} dw + (\varrho_\beta)_{\Delta t}^{r+1}, \\
&= \frac{1}{\Gamma(2-\beta)} \sum_{j=0}^{r} \frac{u(s,t_{j+1}) - 2u(s,t_j) + u(s,t_{j-1})}{\Delta t^2} \int_{t_{r-j+1}}^{t_{r-j}} (\mu)^{-\beta+1} d\mu + (\varrho_\beta)_{\Delta t}^{r+1}, \\
&= \frac{1}{\Gamma(2-\beta)} \sum_{j=0}^{r} \frac{u(s,t_{r-j+1}) - 2u(s,t_{r-j}) + u(s,t_{r-j-1})}{\Delta t^2} \int_{t_{j+1}}^{t_{j+1}} (\mu)^{-\beta+1} d\mu + (\varrho_\beta)_{\Delta t}^{r+1}, \\
&= \frac{1}{\Gamma(3-\beta)} \sum_{j=0}^{r} \frac{u(s,t_{r-j+1}) - 2u(s,t_{r-j}) + u(s,t_{r-j-1})}{\Delta t^\beta} [(j+1)^{2-\beta} - j^{2-\beta}] + (\varrho_\beta)_{\Delta t}^{r+1}, \\
&= \frac{1}{\Gamma(3-\beta)} \sum_{j=0}^{r} \mathrm{q}_j \frac{u(s,t_{r-j+1}) - 2u(s,t_{r-j}) + u(s,t_{r-j-1})}{\Delta t^\beta} + (\varrho_\beta)_{\Delta t}^{r+1} \qquad (2.1)
\end{aligned}$$

where $q_j = (j+1)^{2-\beta} - (j)^{2-\beta}, \mu = (t_{r+1} - w)$ and $(\varrho_\beta)_{\Delta t}^{r+1}$ denotes the associated truncation error.

$$\left|(\varrho_\beta)_{\Delta t}^{r+1}\right| \le \rho_1 (\Delta t)^{2-\beta}, \qquad (2.2)$$

ρ_1 is constant and

- $q_j \in \mathbb{Z}^+, \forall j$
- $1 = q_0 > q_1 > q_2 > q_3 > \cdots > q_r, q_r \to 0$ as $r \to \infty$
- $(2q_0 - q_1) + \sum_{j=1}^{r-1} (-q_{j+1} + 2q_j - q_{j-1}) + (2q_r - q_{r-1}) - q_r = 1$

Similarly,

$$\frac{\partial^{\gamma}}{\partial t^{\gamma}}u(s,t_{r+1}) = \int_{t_0}^{t_{r+1}} \frac{\partial u(s,w)}{\partial w}\frac{(t_{r+1}-w)^{-\gamma}}{\Gamma(1-\gamma)}dw$$

$$= \frac{1}{\Gamma(1-\gamma)}\sum_{j=0}^{r}\int_{t_j}^{t_{j+1}} \frac{\partial u(s,w)}{\partial w}(t_{r+1}-w)^{-\gamma}dw$$

$$= \frac{1}{\Gamma(1-\gamma)}\sum_{j=0}^{r}\frac{u(s,t_{j+1})-u(s,t_j)}{\Delta t}\int_{t_j}^{t_{j+1}}(t_{r+1}-w)^{-\gamma}dw + (\varrho_{\gamma})_{\Delta t}^{r+1}$$

$$= \frac{1}{\Gamma(1-\gamma)}\sum_{j=0}^{r}\frac{u(s,t_{j+1})-u(s,t_j)}{\Delta t}\int_{t_{r-j}}^{t_{r-j+1}}(\mu)^{-\gamma}d\mu + (\varrho_{\gamma})_{\Delta t}^{r+1}$$

$$= \frac{1}{\Gamma(1-\gamma)}\sum_{j=0}^{r}\frac{u(s,t_{r-j+1})-u(s,t_{r-j})}{\Delta t}\int_{t_j}^{t_{j+1}}(\mu)^{-\beta}d\mu + (\varrho_{\gamma})_{\Delta t}^{r+1}$$

$$= \frac{1}{\Gamma(2-\gamma)}\sum_{j=0}^{r}\frac{u(s,t_{r-j+1})-u(s,t_{r-j})}{\Delta t^{\gamma}}[(j+1)^{1-\gamma}-j^{1-\gamma}] + (\varrho_{\gamma})_{\Delta t}^{r+1}$$

$$= \frac{1}{\Gamma(2-\gamma)}\sum_{j=0}^{r} q_j\frac{u(s,t_{r-j+1})-u(s,t_{r-j})}{\Delta t^{\gamma}} + (\varrho_{\gamma})_{\Delta t}^{r+1} \qquad (2.3)$$

where $p_j = (j+1)^{1-\gamma} - (j)^{1-\gamma}, \mu = (t_{r+1}-w)$ and $(\varrho_{\gamma})_{\Delta t}^{r+1}$ denotes the associated truncation error.

$$\left|(\varrho_{\gamma})_{\Delta t}^{r+1}\right| \leq \rho_2(\Delta t)^{1-\gamma} \qquad (2.4)$$

ρ_2 is constant and

- $p_j \in \mathbb{Z}^+, \forall j$
- $1 = p_0 > p_1 > p_2 > p_3 > \cdots > p_r, p_r \to 0$ as $r \to \infty$
- $\sum_{j=0}^{r}(p_j - p_{j+1}) + p_{r+1} = (p_0 - p_1) + \sum_{j=1}^{r-1}(p_j - p_{j+1}) + p_r = 1$

Put (2.1) and (2.3) in (1.1) at $t = t_{r+1}$

$$\sum_{j=0}^{r} q_j\frac{u(s,t_{r-j+1})-2u(s,t_{r-j})+u(s,t_{r-j-1})}{\Delta t^{\beta}\Gamma(3-\beta)} + \sum_{j=0}^{r} p_j\frac{u(s,t_{r-j+1})-u(s,t_{r-j})}{\Delta t^{\gamma}\Gamma(2-\gamma)} + \alpha_1 u(s,t_{r+1})$$

$$-\alpha_2\frac{\partial^2}{\partial s^2}u(s,t_{r+1}) = f(s,t_{r+1}), \quad r = 0,1,2,\ldots\ldots R \qquad (2.5)$$

Applying theta-weighted scheme for $\theta = 1$, Eq. (2.5)

$$\beta_1\sum_{j=0}^{r} q_j(u^{r-j+1} - 2u^{r-j} + u^{r-j-1}) + \gamma_1\sum_{j=0}^{r} p_j(u^{r-j+1} - u^{r-j}) + \alpha_1 u^{r+1} - \alpha_2(u_{ss})^{r+1} = f^{r+1}$$

$r = 0,1,2,3,\ldots\ldots\ldots R$ (2.6)

Where $\beta_1 = \frac{1}{\Delta t^{\beta}\Gamma(3-\beta)}, \gamma_1 = \frac{1}{\Delta t^{\gamma}\Gamma(2-\gamma)}, u(s,t_{r+1}) = u^{r+1}.$

For $r = 0$, the term u^{-1} appears in Eq. (2.6). By applying the initial conditions and substitute $u^{-1} = u^0 - \Delta t\phi_2(s)$ to get the following equation

$$(\beta_1 + \gamma_1 + \alpha_1)u^1 - \alpha_2(u_{ss})^1 = (\beta_1 + \gamma_1)u^0 + \beta_1\Delta t\phi_2(s) + f^1 \qquad (2.7)$$

For $r = 1,2, \dots, R$, Eq. (2.6) is reformed as

$$(\beta_1 + \gamma_1 + \alpha_1)u^{r+1} - \alpha_2(u_{ss})^{r+1} = (2\beta_1 + \gamma_1)u^r - \beta_1 \sum_{j=1}^{r} q_j\left(u^{r-j+1} - 2u^{r-j} + u^{r-j-1}\right) - \gamma_1 \sum_{j=1}^{r} p_j\left(u^{r-j+1} - u^{r-j}\right) - \alpha_1 u^{r-1}\Big) + f^{r+1} \quad (2.8)$$

Now, we discretize the spatial domain $[a, b]$ using $M + 1$ uniformly spaced knots $a = s_0, s_1, s_2, \dots, s_M = b$, where $s_m = s_0 + mh, m = 0,1, \dots, M$. We assume that the HCBS (Hybrid Cubic B-Spline) approximation $U(s, t)$ for the exact solution $u(s, t)$ is given by

$$U(s, t) = \varphi(s, t) + \sum_{m=0}^{M} \varpi_m^r(t)\tilde{\kappa}_m(s, \lambda) \quad (2.9)$$

where $\varphi(s, t)$ and $\tilde{\kappa}_m(s, \lambda)$ are defined in (1.5) and (1.6), respectively.

To find the solution at $t = t_1$,The initial solution is given in (B). However, to initiate the main scheme described in eq (2.8) the control points ϖ_i at $t = t_1$ are required. To obtain these, eq (2.9) is substituted into eq (2.7) to get the equations

$$(\beta_1 + \gamma_1 + \alpha_1)\left[\varphi_i^1 + \sum_{m=i-1}^{i+1} \varpi_m^1 \tilde{\kappa}_m(s_i, \lambda)\right] - \alpha_2\left[(\varphi_{ss})_i^1 + \sum_{m=i-1}^{i+1} \varpi_m^1 (\tilde{\kappa}_m)_{ss}(s_i, \lambda)\right] = (\beta_1 + \gamma_1)u_i^0 + \beta_1 \triangle t\phi_2 + f_i^1, \quad i = 0,1,2 \dots \dots \dots \dots, M \quad (2.10)$$

Solving eq (2.10), we get $[\varpi_0^1, \varpi_1^1, \dots, \varpi_M^1]^T$ and put these control points into eq (2.9) to obtain the estimated solution at $t = t_1$.

Now, find out the Solution at $t = t_{r+1}, r = 1,2. \dots . R$, Using (2.9) in Eq. (2.8), we obtain

$$(\beta_1 + \gamma_1 + \alpha_1)\left[\varphi_i^{r+1} + \sum_{m=i-1}^{i+1} \varpi_m^{r+1} \tilde{\kappa}_m(s_i, \lambda)\right] - \alpha_2\left[(\varphi_{ss})_i^{r+1} + \sum_{m=i-1}^{i+1} \varpi_m^{r+1} (\tilde{\kappa}_m)_{ss}(s_i, \lambda)\right]$$
$$= (2\beta_1 + \gamma_1)\left[\varphi_i^r + \sum_{m=i-1}^{i+1} \varpi_m^r \tilde{\kappa}_m(s_i, \lambda)\right] - \beta_1 \sum_{j=1}^{r} q_j \left[\varphi_i^{r-j+1} - 2\varphi_i^{r-j} + \varphi_i^{r-j-1} + \sum_{m=i-1}^{i+1} \left(\varpi_m^{r-j+1} - 2\varpi_m^{r-j} + \varpi_m^{r-j-1}\right)\tilde{\kappa}_m(s_i, \lambda)\right] - \gamma_1 \sum_{j=1}^{r} p_j \left[\varphi_i^{r-j+1} - \varphi_i^{r-j} + \sum_{m=i-1}^{i+1} \left(\varpi_m^{r-j+1} - \varpi_m^{r-j}\tilde{\kappa}_m(s_i, \lambda)\right]\right.$$
$$\left. - \beta_1\left[(\varphi_i)_i^{r-1} + \sum_{m=i-1}^{i+1} \varpi_m^{r-1}(\tilde{\kappa}_m) \quad (s_i, \lambda)\right] + f_i^{r+1} \qquad i = 0,1,2,3 \dots \dots M \quad (2.11)$$

Equation (2.11) constitutes a linear system comprising $(M + 1)$ equations with an equal number of unknowns, namely the coefficients ϖ_i^{r+1}. Solving this system yields the values of ϖ_i^{r+1} , which are then substituted into Equation (2.9) to compute the approximate solution at the $(r + 1)$th time leve

3. Stability Analysis of Proposed Approach

To analyze the stability of the proposed numerical method, we used Fourier method. Let ϱ_m^r and $\tilde{\varrho}_m^r$ represent the exact and approximate Fourier growth factor. We define the error term ε_m^r as

$$\varepsilon_m^r = \varrho_m^r - \tilde{\varrho}_m^r, m = 1:1:M-1, r = 0:1:R \quad (3.1),$$

Here $\varepsilon^r = [\varepsilon_1^r, \varepsilon_2^r, \dots, \varepsilon_{M-1}^r]^T$. Using (3.1) in (2.11), the equation of error at $(r+1)$ time level is given by

$$(\beta_1 + \gamma_1 + \alpha_1)[c_1\varepsilon_{m-1}^{r+1} + c_2\varepsilon_m^{r+1} + c_1\varepsilon_{m+1}^{r+1}] - \alpha_2[c_4\varepsilon_{m-1}^{r+1} + c_5\varepsilon_m^{r+1} + c_4\varepsilon_{m+1}^{r+1}]$$
$$= (2\beta_1 + \gamma_1)[c_1\varepsilon_{m-1}^{r} + c_2\varepsilon_m^{r} + c_1\varepsilon_{m+1}^{r}] - \beta_1\sum_{j=1}^{r} q_j\big[c_1\big(\varepsilon_{m-1}^{r-j+1} - 2\varepsilon_{m-1}^{r-j} + \varepsilon_{m-1}^{r-j-1}\big)$$
$$+ c_2\big(\varepsilon_m^{r-j+1} - 2\varepsilon_m^{r-j} + \varepsilon_m^{r-j-1}\big) + c_1\big(\varepsilon_{m+1}^{r-j+1} - 2\varepsilon_{m+1}^{r-j} + \varepsilon_{m+1}^{r-j-1}\big)\big] - \gamma_1\sum_{j=1}^{r} p_j\big[c_1\big(\varepsilon_{m-1}^{r-j+1} - \varepsilon_{m-1}^{r-j}\big)$$
$$+ c_2\big(\varepsilon_m^{r-j+1} - \varepsilon_m^{r-j}\big) + c_1\big(\varepsilon_{m+1}^{r-j-1} - \varepsilon_{m+1}^{r-j}\big) - \beta_1\big(c_1\varepsilon_{m-1}^{r-1} + c_2\varepsilon_m^{r-1} + c_1\varepsilon_{m+1}^{r-1}\big),$$
$$m = 1,2,3,,M-1 \qquad (3.2)$$

If $\varepsilon_m^r = \varrho^r e^{\iota u m h}$, where $\iota = \sqrt{-1}$ and $u = \frac{2\pi m}{b-a}$, then (3.2) is reshaped as

$$[(\beta_1 + \gamma_1 + \alpha_1)(2c_1\cos uh + c_2) - \alpha_2(2c_4\cos uh + c_5)]\varrho^{r+1} = \alpha_4[2c_1\cos uh + c_2]\varrho^r$$
$$-\beta_1(2c_1\cos uh + c_2)\sum_{j=1}^{r} q_j\big[\varrho^{r-j+1} - 2\varrho^{r-j} + \varrho^{r-j-1}\big] - \gamma_1(2c_1\cos uh + c_2)\sum_{j=1}^{r} p_j\big[\varrho^{r-j+1} - \varrho^{r-j}\big]$$
$$- \beta_1(2c_1\cos uh + 2)\varrho^{r-1} \qquad (3.3)$$

After solving (3.3), we get the following result

$$\varrho^{r+1} = \frac{1}{\mathrm{H}}\left[(1+\mathrm{H}_1)\varrho^r - \mathrm{H}_1\sum_{j=1}^{r} q_j\big[\varrho^{r-j+1} - 2\varrho^{r-j} + \varrho^{r-j-1}\big] - \mathrm{H}_2\sum_{j=1}^{r} p_j\big[\varrho^{r-j+1} - \varrho^{r-j}\big] - \mathrm{H}_1\varrho^{r-1}\right] \quad (3.4)$$

where $\mathrm{H} = 1 + \mathrm{H}_3 + \frac{12\mathrm{H}_4(2+\lambda)\sin^2(uh/2)}{h^2[6+(4-\lambda)\sin^2(uh/2)]} \geq 1, \mathrm{H}_1 = \frac{\beta_1}{\beta_1+\gamma_1}, \mathrm{H}_2 = \frac{\gamma_1}{\beta_1+\gamma_1}, \mathrm{H}_3 = \frac{\alpha 1}{\beta_1+\gamma_1}$ and $\mathrm{H}_4 = \frac{\alpha 2}{\beta_1+\gamma_1}$.

For $r = 0$, the eq (3.3) takes the following form

$$|\varrho^1| = \tfrac{1}{\mathrm{H}}|(1+\mathrm{H}_1)\varrho^0| \leq (1+\mathrm{H}_1)|\varrho^0|, \because \mathrm{H} \geq 1.$$

Now, assuming $|\varrho^r| \leq (1+\mathrm{H}_1)|\varrho^0|$ for $r > 1$, we use eq (3.4) to continue as

$$|\varrho^{r+1}| = \tfrac{1}{\mathrm{H}}\big[(1+\mathrm{H}_1)|\varrho^r| - \mathrm{H}_1\textstyle\sum_{j=1}^{r} q_j\big[|\varrho^{r-j+1}| - 2|\varrho^{r-j}| + \varrho^{r-j-1}\big] - \mathrm{H}_2\sum_{j=1}^{r} p_j\big[|\varrho^{r-j+1}| - |\varrho^{r-j}|\big] - \mathrm{H}_1|\varrho^{r-1}|\big]$$
$$\leq (1+\mathrm{H}_1)^2|\varrho^0| - \mathrm{H}_1(1+\mathrm{H}_1)\textstyle\sum_{j=1}^{r} q_j[|\varrho^0| - 2|\varrho^0| + \varrho^0] - \mathrm{H}_2(1+\mathrm{H}_1)\sum_{j=1}^{r} p_j[|\varrho^0| - |\varrho^0|] - \mathrm{H}_1(1+\mathrm{H}_1)|\varrho^0|$$
$$= (1+\mathrm{H}_1)^2|\varrho^0| - \mathrm{H}_1(1+\mathrm{H}_1)|\varrho^0|$$
$$= (1+\mathrm{H}_1)[1+\mathrm{H}_1-\mathrm{H}_1]|\varrho^0|$$
$$\Rightarrow |\varrho^{r+1}| \leq (1+\mathrm{H}_1)|\varrho^0|, \forall r.$$

we obtain $|\varepsilon^r| = (1+\mathrm{H}_1)|\varepsilon^0|, r = 0,1,\dots,R$. Therefore, the numerical scheme is stable.

4. Consistency and Convergence Analysis

Let $\widetilde{U}(s,t) = \sum_{m=0}^{M} d_m(t)\tilde{\kappa}_m(s)$ represent the computed HCBS approximation of the numerical solution $U(s,t)$ with the analytical solution denoted by $u(s,t)$. This approximation satisfies the interpolating conditions $L\widetilde{U}(s_m,t) = \tilde{f}(s_m,t), m = 0,1,\dots,M$. The corresponding problem, expressed as a difference equation $L\left(\widetilde{U}(s_m,t) - U(s_m,t)\right)$, at $t = t_r$, is given by

$$(\beta_1 C_1 + \gamma_1 C_1 + \alpha_1 C_1 + \alpha_2 C_4)\omega_{m-1}^{r+1} + (\beta_1 C_2 + \gamma_1 C_2 + \alpha_1 C_2 + \alpha_2 C_5)\omega_m^{r+1}$$
$$+(\beta_1 C_1 + \gamma_1 C_1 + \alpha_1 C_1 + \alpha_2 C_4)\omega_{m+1}^{r+1} = (2\beta_1 + \gamma_1)(C_1\omega_{m-1}^r + C_2\omega_m^r + C_1\omega_{m+1}^r)$$
$$-\beta_1\sum_{k=1}^{r} q_k\left[C_1\left(\omega_{m-1}^{r-k+1} - 2\omega_{m-1}^{r-k} + \omega_{m-1}^{r-k-1}\right) + C_2\left(\omega_m^{r-k+1} - 2\omega_m^{r-k} + \omega_m^{r-k-1}\right)\right.$$
$$\left.+C_1\left(\omega_{m+1}^{r-k+1} - 2\omega_{m+1}^{r-k} + \omega_{m+1}^{r-k-1}\right)\right] - \gamma_1\sum_{k=1}^{r} p_k\left[C_1\left(\omega_{m-1}^{r-k+1} - \omega_{m-1}^{r-k}\right) + C_2\left(\omega_m^{r-k+1} - \omega_m^{r-k}\right)\right.$$
$$\left.+C_1\left(\omega_{m+1}^{r-k+1} - \omega_{m+1}^{r-k}\right)\right] - \beta_1(C_1\omega_{m-1}^{r-1} + C_2\omega_m^{r-1} + C_1\omega_{m+1}^{r-1}) + f_m^{r+1}, \quad m = 0,1,\dots,M \quad (4.1)$$

where $\omega_m^r = \varpi_m^r - d_m^r$ and $l_m^r = h^2\left[f_m^r - \tilde{f}_m^r\right]$.

The boundary conditions can be rephrased as $C_1\omega_{m-1}^{r+1} + C_2\omega_m^{r+1} + C_1\omega_{m+1}^{r+1} = 0, m = 0, M$.

Furthermore, following [38], we have

$$\left\|D^j(u(s,t) - \tilde{U}(s,t))\right\|_\infty \le Z_j h^{4-j}, j = 0,1,2 \quad (4.2),$$

Therefore, $|l_m^r| = h^2\left|f_m^r - \tilde{f}_m^r\right| \le Zh^4$, where Z is independent of the mesh spacing and remains constant with respect to the discretization parameters. Now, we introduce $l^r = \max_{m=0}^{M}\{|l_m^r|\}$, $\tilde{e}_m^r = |\omega_m^r|$ and $\tilde{e}^r = \max_{m=0}^{M}\{|e_m^r|\}$. For $r = 0$, Eq. (4.1) transforms into following relation

$$(\beta_1 C_2 + \alpha_1 C_2 + \alpha_1 C_2 + \alpha_2 C_5)\omega_m^1 = (\beta_1 C_1 + \alpha_2 C_4)(\omega_{m+1}^1 - \omega_{m-1}^1) + (\gamma_1 C_1 + \alpha_1 C_1)(\omega_{m+1}^1 - \omega_{m-1}^1) + \frac{1}{h^2} l_m^1.$$

Involving the absolute values of l_m^r and ω_m^r, we get

$$\tilde{e}_m^1 \le \frac{6Zh^4}{2\beta_1 h^2(2+\lambda) + 12(2+\lambda)\alpha_1 + 6\alpha_2 h}$$

By applying the end constraints, we get $\tilde{e}^1 \le Z_1 h^2$, where Z_1 remains independent of the spatial grid spacing. Now, assuming that $\tilde{e}_m^k \le Z_r h^2$ for $r > 1$, we define $Z = max_{j=0}^{r}\{Z_j\}$ Substituting the absolute values of l_m^r and ω_m^r in Eq. (4.1)

$$\tilde{e}_m^{r+1} \le \frac{6Zh^2}{(\beta_1 + \gamma_1 + \alpha_1)h^2(2+\lambda) - 12(2+\lambda)\alpha_2}[(2\beta_1 + \gamma_1)(C_1\omega_{m-1}^r + C_2\omega_m^r + C_1\omega_{m+1}^r)$$
$$-\beta_1(C_1\omega_{m-1}^{r-1} + C_2\omega_m^{r-1} + C_1\omega_{m+1}^{r-1}) - \left(\beta_1\sum_{j=0}^{r-1}\left(q_{j-1} - 2q_j + q_{j+1}\right)\right.$$
$$\left.+\gamma_1\sum_{j=0}^{r-1}\left(q_{j-1} - q_j\right)\right)Zh^2 + Zh^2\Big].$$

By applying the boundary conditions, we arrive at $\tilde{e}_m^{r+1} \le Zh^2$. Therefore, this result is true for all value of r. Using the result $\sum_{m=0}^{M}|\kappa_m(s,\lambda)| \le 1.75$ [31], we get

$$\|\tilde{U}(s,t) - U(s,t)\|_\infty = \left\|\sum_{m=0}^{M}\left(d_m(t) - \varpi_m(t)\right)\kappa_m(s,\lambda)\right\|_\infty \le 1.75Zh^2 \quad (4.3),$$

Consequently, using (4.2) and (4.3), we get

$$\|u(s,t) - U(s,t)\|_\infty \le \|u(s,t) - \tilde{U}(s,t)\|_\infty + \|\tilde{U}(s,t) - U(s,t)\|_\infty$$
$$\le Z_0 h^4 + 1.75Zh^2.$$

Based on the preceding analysis and using equations (2.2) and (2.4), it can be concluded that the proposed scheme attains second-order accuracy $O(h^2)$ in spatial direction. Furthermore, equations (2.2) and (2.4) also reveal that the truncation error in the temporal direction is of the order $O\left(\Delta t^{2-\beta} + \Delta t^{1-\gamma}\right)$. T This study focuses on a specific class of problems characterized by the relationships $\beta = \gamma + 1$ and $\beta = 2\gamma$. Consequently, the scheme is theoretically $O\left(\Delta t^{2-\beta}\right)$ accurate when $\alpha = 1 + \gamma$ and $O\left(\Delta t^{1-\beta/2}\right)$ when $\beta = 2\gamma$.

5. Numerical Results and Discussion.

To assess the accuracy of the proposed method, a series of numerical experiments are performed. The following error norms are utilized to quantify the approximation errors:

$$L_\infty = \max_{m=0}^{M} |U_m - u_m|, L_2 = \sqrt{h \sum_{m=0}^{M} |U_m - u_m|^2},$$

In addition, the experimental order of convergence (EOC) is computed using the following standard formula [37]

$$\text{Eoc} = \frac{1}{\log 2} \log\left[\frac{L_\infty(2m)}{L_\infty(m)}\right],$$

6. Numerical Problems.

Problem No. 6.1

Consider the TFTE of the form [18]

$$\frac{\partial^{2\beta} u(s,t)}{\partial t^{2\beta}} + \frac{\partial^{\beta} u(s,t)}{\partial t^{\beta}} = \frac{\partial^2 u(s,t)}{\partial s^2} + f(s,t) \quad \text{, for all } (s,t) \in [0,1] \times [0,1],$$

where,

$$f(s,t) = \sin(s)\left[6t + 6\frac{t^{3-\beta}}{\Gamma(4-\beta)} + 2(t^3 + 1)\right]$$

where the initial and boundary conditions are

$$u(s,0) = 0, \qquad u_t(s,0) = 0\,, \qquad u(0,t) = 0, \qquad u(1,t) = 0$$

Exact solution $u(s,t) = t^{2+\beta} \sin(2\pi s)$ [18].

Table 1 displays the absolute numerical errors obtained using the HCBS method for the problem, with a time step size of Δt = 0.025 and β = 0.5, evaluated at various spatial grid points. In Table 2, we compute the convergence order, as discussed in [18], and report the maximum absolute errors for different combinations of temporal and spatial step size $h = 5, \tau = 1/M, (M = 20, 40, 80)$. The L2-norm and the maximum errors are presented for β values of 0.6, 0.7, 0.8, and 0.9. Table 3 summarizes the maximum absolute error and the observed convergence order for β = 0.75 and τ = 1/100.

Additionally, the piecewise approximate solution to Problem 6.1, derived using the proposed numerical scheme, is provided. $\beta = 0.5, \quad 0 \le s \le 1, \quad N = 40, \quad \Delta t = 0.025.$

$$f(s)=\begin{cases}-4.63096\times10^{-21}+s\left(1.99754+s(-0.0678009+s(1.27488-6.53823s))\right), & s\in[0.00,0.05]\\ -0.034288+s\left(2.69241+s(-5.00091+s(14.9866-16.862s))\right), & s\in[0.05,0.10]\\ -0.574781+s\left(8.18877+s(-24.6293+s(42.6022-27.6675s))\right), & s\in[0.10,0.15]\\ -3.23164+s\left(26.1606+s(-67.2561+s(82.2811-37.7756s))\right), & s\in[0.15,0.20]\\ -11.2861+s\left(66.8943+s(-139.333+s(132.053-46.9537s))\right), & s\in[0.20,0.25]\\ -29.9022+s\left(141.889+s(-244.716+s(189.38-54.9758s))\right), & s\in[0.25,0.30]\\ -65.9339+s\left(262.164+s(-384.178+s(251.274-61.6441s))\right), & s\in[0.30,0.35]\\ -127.276+s\left(436.376+s(-555.071+s(314.407-66.7946s))\right), & s\in[0.35,0.40]\\ -221.761+s\left(668.899+s(-751.178+s(375.237-70.3003s))\right), & s\in[0.40,0.45]\\ -355.635+s\left(958.002+s(-962.771+s(430.145-72.0751s))\right), & s\in[0.45,0.50]\\ -531.719+s\left(1294.3+s(-1176.86+s(475.577-72.0751s))\right), & s\in[0.50,0.55]\\ -747.382+s\left(1659.58+s(-1377.67+s(508.183-70.3003s))\right), & s\in[0.55,0.60]\\ -992.505+s\left(2026.23+s(-1547.27+s(524.959-66.7946s))\right), & s\in[0.60,0.65]\\ -1247.64+s\left(2357.2+s(-1666.4+s(523.369-61.6441s))\right), & s\in[0.65,0.70]\\ -1482.58+s\left(2606.78+s(-1715.39+s(501.466-54.9758s))\right), & s\in[0.70,0.75]\\ -1655.55+s\left(2722.08+s(-1675.26+s(457.986-46.9537s))\right), & s\in[0.75,0.80]\\ -1713.29+s\left(2645.29+s(-1528.75+s(392.421-37.7756s))\right), & s\in[0.80,0.85]\\ -1592.06+s\left(2316.62+s(-1261.52+s(305.078-27.6675s))\right), & s\in[0.85,0.90]\\ -1218.77+s\left(1676.31+s(-862.284+s(196.908-16.862s))\right), & s\in[0.90,0.95]\\ -591.748+s\left(771.586+s(-375.231+s(80.8869-6.53823s))\right), & s\in[0.95,1.00]\end{cases}$$

Table.1 Exact and Approximate solution for Problem 6.1 with $\Delta t = 0.025$, and $\beta = 0.5$

s	Exact Solution	Approximate Solution	Error
0	0	0	0
0.0785398	0.156918	0.156918	2.51982×10^{-12}
0.392699	0.765367	0.765367	1.22896×10^{-11}
0.628319	1.17557	1.17557	1.88769×10^{-11}
0.863938	1.52081	1.52081	2.44256×10^{-11}
1.09956	1.78201	1.78201	2.86187×10^{-11}
1.33518	1.94474	1.94474	3.12346×10^{-11}
1.5708	2	2	3.21232×10^{-11}
1.88496	1.90211	1.90211	3.05469×10^{-11}
2.04204	1.78201	1.78201	2.73861×10^{-11}
2.27765	1.52081	1.52081	2.44249×10^{-11}
2.59181	1.045	1.045	1.67819×10^{-11}

2.98451	0.312869	0.312869	5.02354×10^{-12}
3.06305	0.156918	0.156918	2.51948×10^{-12}
3.14159	0	0	0

Table.2 A comparison of maximum absolute error with h = 5τ = 1/M at T = 1 for Problem 6.1.

β	L^{∞}-norm [18]			L^{∞}-norm proposed method		
	$M_1 = 20$	$M_2 = 40$	$M_3 = 80$	$M_1 = 20$	$M_2 = 40$	$M_3 = 80$
0.6	2.6718E-03	1.2924E-03	2.3578E-04	2.5731E-04	6.3948E-05	3.0179E-05
0.7	1.1386E-03	3.0011E-04	7.4367E-05	8.1732E-05	2.4950E-05	7.5438E-06
0.8	8.5605E-04	7.3477E-05	4.8225E-06	5.9224E-06	2.0075E-06	6.2091E-07
0.9	2.8284E-05	4.5304E-06	3.4472E-07	9.3649E-07	5.7704E-07	6.8459E-08

Table.3 Maximum absolute error and Order of Convergence for Problem 6.1.

N	Method [18]			Proposed Method		
	L∞-norm	L2-norm	EOC	L∞-norm	L2-norm	EOC
05	4.5584E-04	3.3892E-04	...	8.2976E-05	6.3009E-05	...
10	9.1361E-05	6.7926E-05	2.31889	3.3457E-06	2.1278E-06	1.95
20	1.5847E-05	1.1206E-05	2.52731	5.4148E-06	4.9018E-06	2.07
40	9.2497E-07	6.5406E-07	4.09870	8.2537E-07	3.7193E-07	1.97

Figure. 1 Exact and Approximate solution at different time level for Problem 6.1.

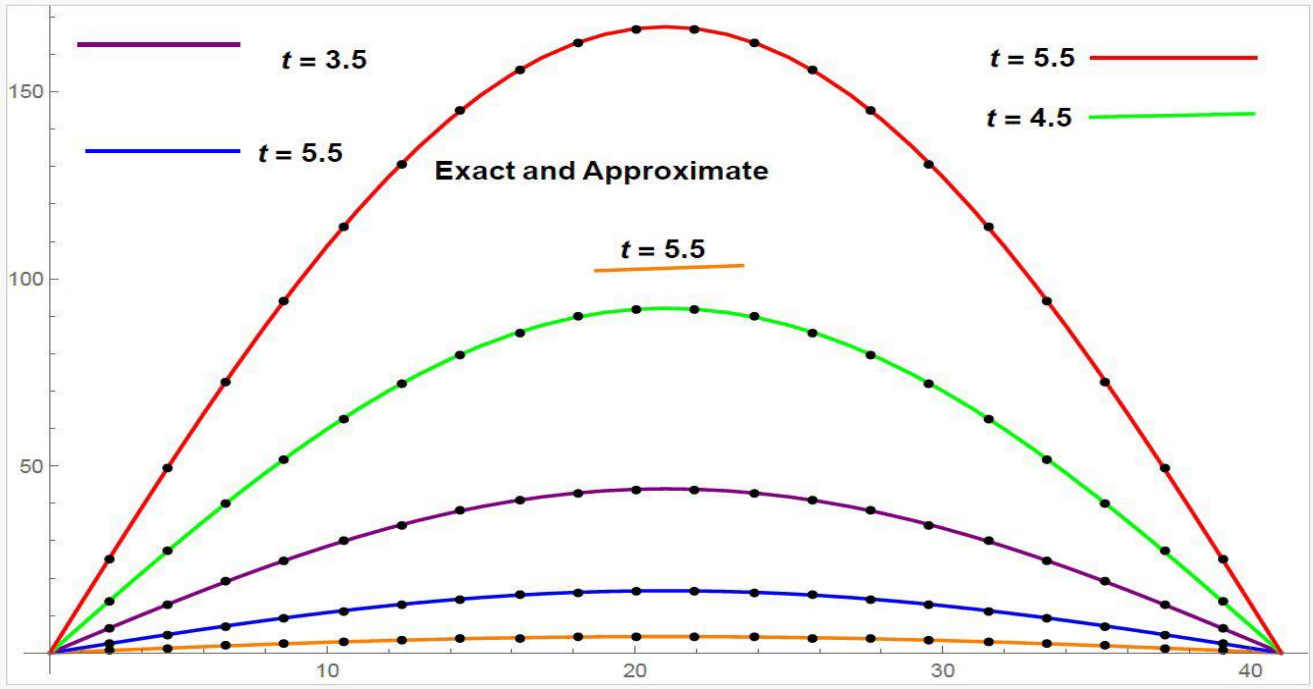

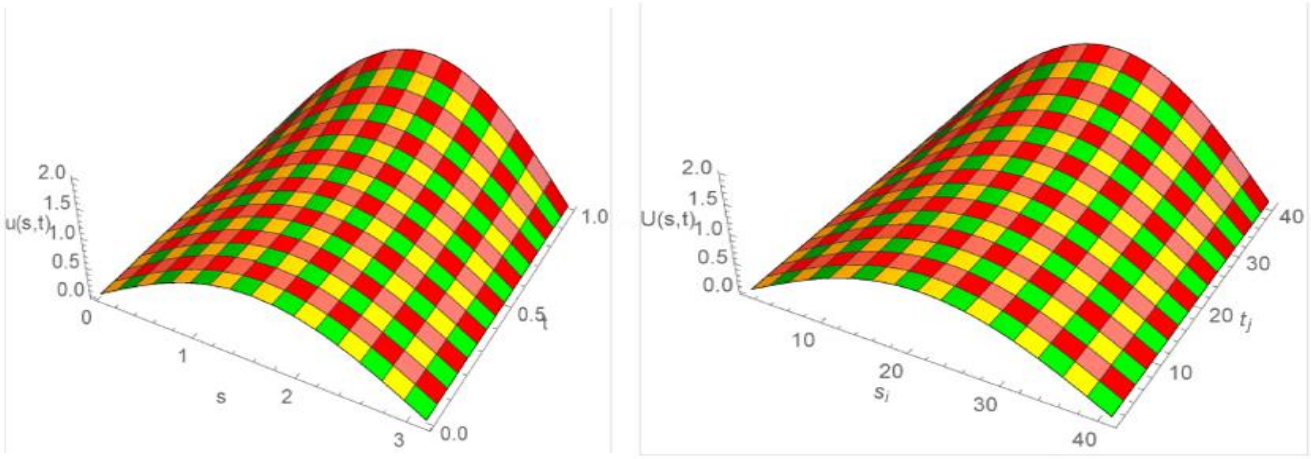

Figure. 2. Plot of Exact and Approximate solution for problem 6.1

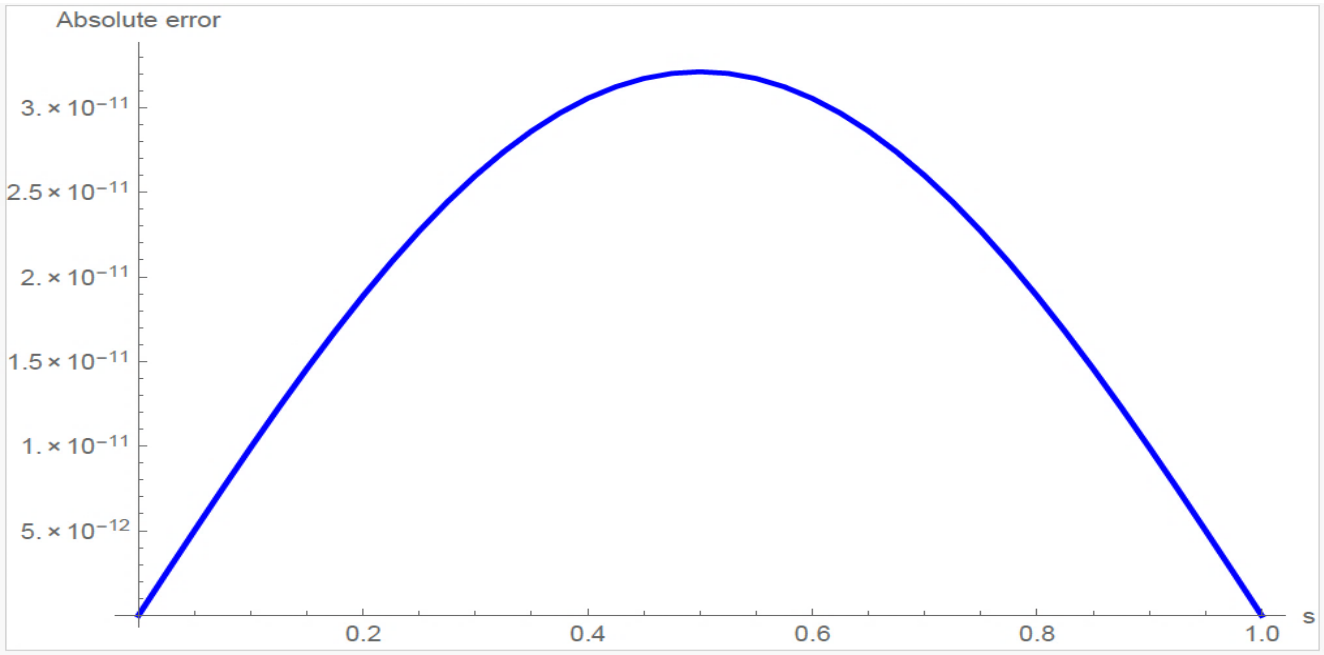

Figure. 3 Plot for Absolute error for Problem 6.1.

Problem No.6.2

Consider the following fractional telegraph partial differential equation [32]

$$\frac{\partial^2 u(s,t)}{\partial s^2}+\frac{\partial^\beta u(s,t)}{\partial s^\beta}-\frac{\partial^2 u(s,t)}{\partial t^2}+6u(s,t)=6(t^2-3t+2)\left(s^3+s+1+\frac{s^{3-\beta}}{\Gamma(4-\beta)}\right)-2(s^3+1)$$

$1<t<2,\quad 0<s<\pi,\quad 0\le\beta\le 1,\quad \lambda=1,$

$u(0,t)=t^2-3t+2,\quad u_s(0,t)=0,\quad 0\le s\le 1$

$u(s,\pi)=u(s,2)=0,\quad 1\le t\le 2$

Exact solution= $u(s,t)=(s^3+1)(t^2-3t+2)$ [32]

Table.4 displays the exact and approximate solution with $\Delta t = 0.01,\ and\ \beta = 0.5$ It show the absolute numerical errors obtained using the HCBS method for the problem, with a time step size of Δt = 0.01 and β = 0.5, evaluated at various spatial grid points. In Table.5, we compute the maximum absolute errors for different combinations of $spatial\ and\ temporal\ step\ size\ h = 1/M, \tau = 1/N, (N = 4, 8, 12)$. The L^{∞}-norm and the maximum errors are presented for β values of 0.64, 0.8 and 0.96. Table 6 summarizes the maximum absolute error with different value of β(0.64,0.80,0.96) and N (4,8,12). Additionally, the piecewise approximate solution to Problem 6.2, derived using the proposed numerical scheme, is provided. $\beta = 0.5, \quad 0 \le s \le \pi, \quad N = 20, \quad \Delta t = 0.01.$

$$f(s) = \begin{cases} -1.08366 \times 10^{-18} + s(1.99631 + s(-0.0679719 + s(1.2779 - 6.54862s))), & s \in \left[0, \frac{\pi}{20}\right] \\ -0.0343336 + s(2.69209 + s(-5.00749 + s(15.0069 - 16.8841s))), & s \in \left[\frac{\pi}{20}, \frac{2\pi}{20}\right] \\ -0.575524 + s(8.19554 + s(-24.6611 + s(42.658 - 27.7033s))), & s \in \left[\frac{2\pi}{20}, \frac{3\pi}{20}\right] \\ -3.23582 + s(26.1906 + s(-67.343 + s(82.3882 - 37.8245s))), & s \in \left[\frac{3\pi}{20}, \frac{4\pi}{20}\right] \\ -11.3007 + s(66.977 + s(-139.513 + s(132.224 - 47.0145s))), & s \in \left[\frac{4\pi}{20}, \frac{5\pi}{20}\right] \\ -29.9409 + s(142.069 + s(-245.032 + s(189.625 - 55.047s))), & s \in \left[\frac{5\pi}{20}, \frac{6\pi}{20}\right] \\ -66.0192 + s(262.499 + s(-384.675 + s(251.599 - 61.7239s))), & s \in \left[\frac{6\pi}{20}, \frac{7\pi}{20}\right] \\ -127.441 + s(436.937 + s(-555.789 + s(314.814 - 66.8811s))), & s \in \left[\frac{7\pi}{20}, \frac{8\pi}{20}\right] \\ -222.048 + s(669.76 + s(-752.15 + s(375.723 - 70.3914s))), & s \in \left[\frac{8\pi}{20}, \frac{9\pi}{20}\right] \\ -356.095 + s(959.237 + s(-964.016 + s(430.702 - 72.1684s))), & s \in \left[\frac{9\pi}{20}, \frac{10\pi}{20}\right] \\ -532.406 + s(1295.97 + s(-1178.38 + s(476.193 - 72.1684s))), & s \in \left[\frac{10\pi}{20}, \frac{11\pi}{20}\right] \\ -748.348 + s(1661.73 + s(-1379.46 + s(508.841 - 70.3914s))), & s \in \left[\frac{11\pi}{20}, \frac{12\pi}{20}\right] \\ -993.788 + s(2028.85 + s(-1549.27 + s(525.638 - 66.8811s))), & s \in \left[\frac{12\pi}{20}, \frac{13\pi}{20}\right] \\ -1249.25 + s(2360.24 + s(-1668.55 + s(524.046 - 61.7239s))), & s \in \left[\frac{13\pi}{20}, \frac{14\pi}{20}\right] \\ -1484.49 + s(2610.14 + s(-1717.61 + s(502.115 - 55.047s))), & s \in \left[\frac{14\pi}{20}, \frac{15\pi}{20}\right] \\ -1657.69 + s(2725.6 + s(-1677.42 + s(458.578 - 47.0145s))), & s \in \left[\frac{15\pi}{20}, \frac{16\pi}{20}\right] \\ -1715.5 + s(2648.71 + s(-1530.73 + s(392.928 - 37.8245s))), & s \in \left[\frac{16\pi}{20}, \frac{17\pi}{20}\right] \\ -1594.11 + s(2319.61 + s(-1263.14 + s(305.472 - 27.7033s))), & s \in \left[\frac{17\pi}{20}, \frac{18\pi}{20}\right] \\ -1220.35 + s(1678.48 + s(-863.406 + s(197.165 - 16.8841s))), & s \in \left[\frac{18\pi}{20}, \frac{19\pi}{20}\right] \\ -592.672 + s(772.787 + s(-375.818 + s(81.0145 - 6.54862s))), & s \in \left[\frac{19\pi}{20}, \pi\right] \end{cases}$$

Table.4 Exact and Approximate solution for Problem 6.2 with $\Delta t = 0.01$, $and\ \beta = 0.5$

s	Exact Solution	Approximate Solution	Error
0	0	2.2804×10^{-21}	2.2804×10^{-21}
0.3142	0.6180	0.6180	1.2653×10^{-12}
0.9425	1.6180	1.6180	3.2991×10^{-12}
1.0996	1.7820	1.7820	3.6338×10^{-12}
1.5708	2.0000	2.0000	4.0807×10^{-12}
1.8849	1.9021	1.9021	3.8817×10^{-12}
2.0421	1.7820	1.7820	3.6351×10^{-12}
2.6704	0.9079	0.9079	1.8585×10^{-12}
2.9845	0.3129	0.3129	6.4079×10^{-13}
3.1416	0	2.2804×10^{-21}	2.2804×10^{-21}

Table.5 A comparison of maximum absolute error with different value of β and N for Problem 6.2.

β	L^{∞}-norm [18]			L^{∞}-norm proposed method		
	$N_1 = 4$	$N_2 = 8$	$N_3 = 12$	$N_1 = 4$	$N_2 = 8$	$N_3 = 12$
0.64	7.1338E-04	4.7991E-05	2.0456E-05	3.7187E-06	8.3749E-07	7.0011E-07
0.80	9.1888E-04	2.1761E-04	8.4596E-05	6.1592E-06	9.5609E-07	8.7192E-07
0.96	3.4712E-03	9.9306E-04	4.2966E-04	5.8168E-05	2.0135E-06	2.1285 E-06

Table.6 A Comparison of L^2-Norm with with different value of β and N for Problem 6.2.

β	L^2-Norm [18]			L^2-Norm proposed method		
	$N_1 = 4$	$N_2 = 8$	$N_3 = 12$	$N_1 = 4$	$N_2 = 8$	$N_3 = 12$
0.64	4.6717E-04	2.5237E-05	1.2217E-05	4.3291E-06	9.1238E-07	7.9937E-07
0.80	6.6621E-04	1.4636E-04	5.6376E-05	3.0219E-06	6.4133E-07	7.2245E-07
0.96	2.5836E-03	6.6448E-04	2.8157E-04	6.9109E-05	3.4871E-06	3.0729E-06

Figure.4 Plot of the approximated and Exact Solution for Problem 6.2

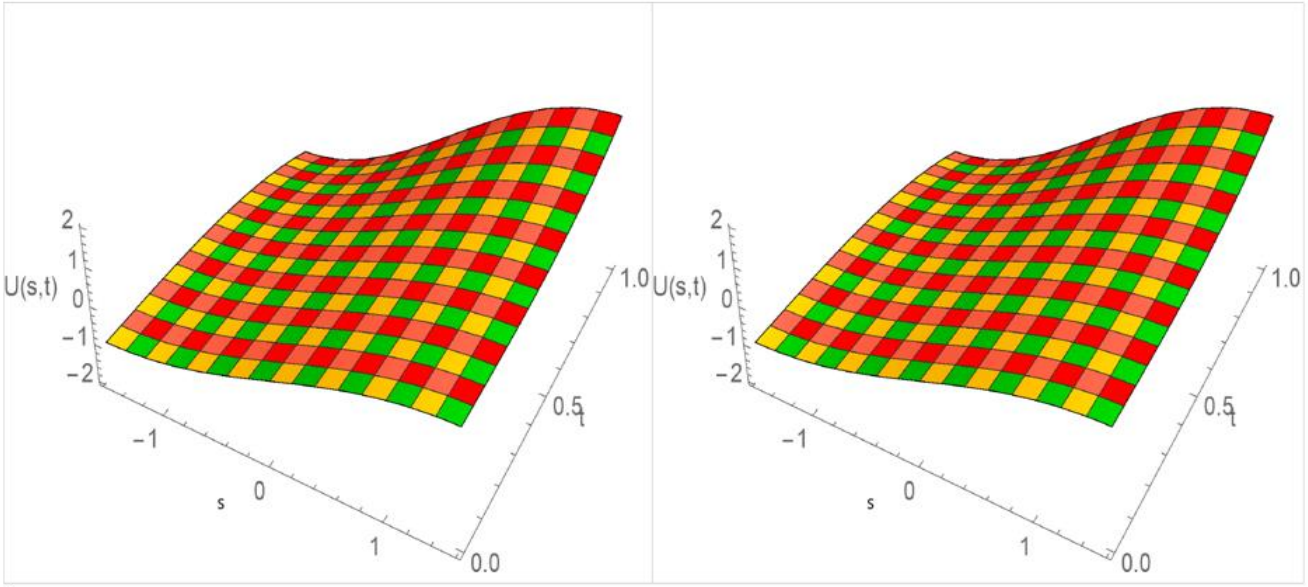

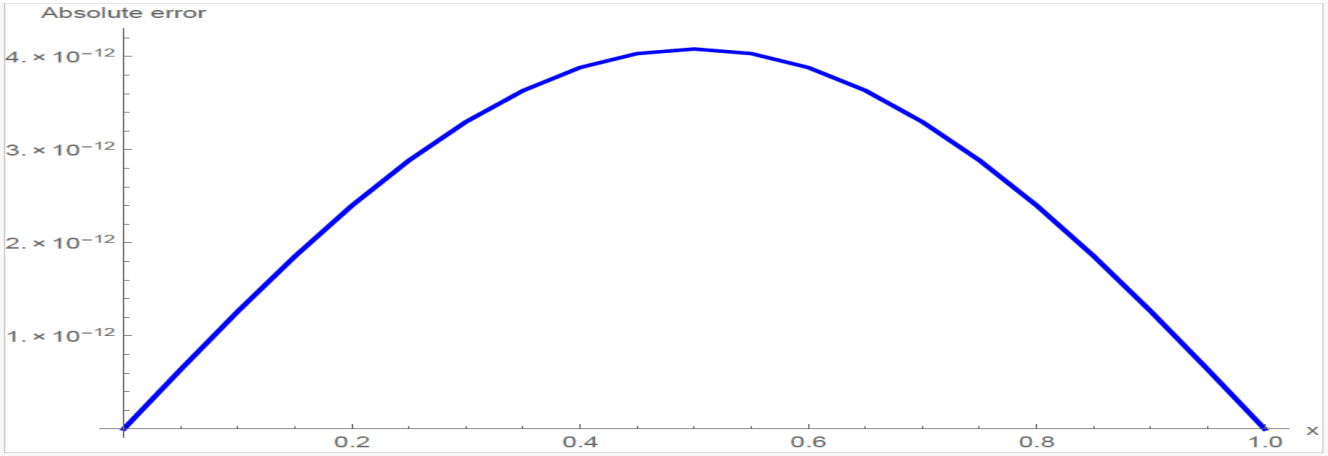

Figure .5 Plot of Absolute error for Problem 6.2

Problem No.6.3

Take the one-dimensional time fractional telegraph equation with $\beta = \frac{2}{3}$, [35]

$$ {}_cD_t^{2\beta}u(s,t) + {}_cD_t^{\beta}u(s,t) = D_s^2u(s,t) + f(s,t), 0 < s < 1, 0 < t \leq 1,$$

Where,

$$f(s,t) = 6\sin(s+1)\left(\frac{t^{3-2\beta}}{\Gamma(4-2\beta)} + \frac{t^{3-\beta}}{\Gamma(4-\beta)}\right) + \sin(s+1)(t^3+1)$$

subject to the initial condition

$$u(s,0) = \sin(s+1), u_t(s,0) = 0, 0 < s < 1,$$

and the boundary conditions

$$u(0,t) = \sin(1)(t^3+1), 0 < t \leq 1$$
$$u(1,t) + 3u_s(1,t) = (t^3+1)(\sin(2) + 3\cos(2)), 0 < t \leq 1$$

Exact solution = $u(s,t) = (t^3+1)\sin(s+1)$ [35].

Table.7 displays the exact and approximate solution with N=50.In Table.8 we compute the maximum absolute error at t = 1, β = 2/3, N = 50 and M (10,20,35,50,70,90). Table. 9 summarizes the maximum absolute error for different M, N, n and β= 2/3 at t = 1.

Additionally, the piecewise approximate solution to Problem 6.3, derived using the proposed numerical scheme, is provided. $\beta = 2/3, \quad 0 \leq s \leq 1, \quad N = 50, \quad \Delta t = 0.02.$

$$f(s) = \begin{cases} 55824. + s(111057. + s(73648.9 + (16279.8 + 1.35939 \times 10^{-8}s)s)), & s \in [0.00, 0.02] \\ -4.54747 \times 10^{-11} + s(-1. + s(1. + (-5.18412 \times 10^{-11} - 8.8656 \times 10^{-12}s)s)), & s \in [0.02, 0.04] \\ -3.81988 \times 10^{-11} + s(-1. + s(1. + (-4.72937 \times 10^{-11} - 8.8656 \times 10^{-12}s)s)), & s \in [0.04, 0.06] \\ \vdots & \vdots \\ -4.1382 \times 10^{-11} + s(-1. + s(1. + (5.20686 \times 10^{-11} - 8.8656 \times 10^{-12}s)s)), & s \in [0.96, 0.98] \\ 12394.7 + s(-24659.4 + s(16353.1 + (-3614.61 + 3.01137 \times 10^{-9}s)s)), & s \in [0.98, 1.00] \end{cases}$$

Table.7 Exact and Approximate Solution for Problem 6.3 with N=50.

x	Exact Solution	Approximate Solution	Error
-1.5708	4.0382	4.0382	8.88178×10^{-16}
-1.50796	3.78192	3.78192	3.10862×10^{-15}

-1.00531	2.01596	2.01596	1.28786×10^{-14}
-0.942478	1.83074	1.83074	1.33227×10^{-14}
-0.0628319	0.0667797	0.0667797	1.16851×10^{-14}
0	0	-1.14717×10^{-14}	1.14717×10^{-14}
0.0628319	-0.058884	-0.058884	1.12757×10^{-14}
0.942478	-0.0542134	-0.0542134	9.29812×10^{-15}
1.00531	0.00533784	0.00533784	9.05352×10^{-15}
1.5708	0.896605	0.896605	1.11022×10^{-16}

Table.8 The maximum absolute error for Problem 6.3 at t = 1, β = 2/3, N = 50)

M	L∞ [35]	L∞ (Proposed method)
10	1.8374×10^{-4}	7.3104×10^{-10}
20	0.3122×10^{-4}	5.2149×10^{-11}
35	0.0373×10^{-4}	4.3897×10^{-11}
50	0.0075×10^{-4}	3.2220×10^{-11}
70	4.1355×10^{-4}	2.2545×10^{-11}
90	6.0201×10^{-5}	8.3792×10^{-12}

Table.9 The maximum absolute error for different M, N, n and β for Problem 6.3 at $t = 1$

	Method [35]			Proposed Method		
M	α = 1.25	α = 1.5	α = 1.95	α = 1.25	α = 1.5	α = 1.95
5	1.0734	1.0734	1.0734	8.3137×10^{-8}	8.3137×10^{-8}	8.3137×10^{-8}
7	0.0242	0.0242	0.0242	7.2134×10^{-8}	7.2134×10^{-8}	7.2134×10^{-8}
10	0.0086	0.0086	0.0086	9.9149×10^{-9}	9.9149×10^{-9}	9.9149×10^{-9}
20	9.4927e-005	9.4845e-005	9.4650e-005	6.0157×10^{-10}	6.0157×10^{-10}	6.0157×10^{-10}
30	1.8743e-005	1.8332e-005	1.7310e-005	7.2148×10^{-11}	7.2146×10^{-11}	7.2146×10^{-11}
50	1.1274e-005	1.0852e-005	9.8078e-006	9.5037×10^{-12}	9.5037×10^{-12}	9.5037×10^{-12}

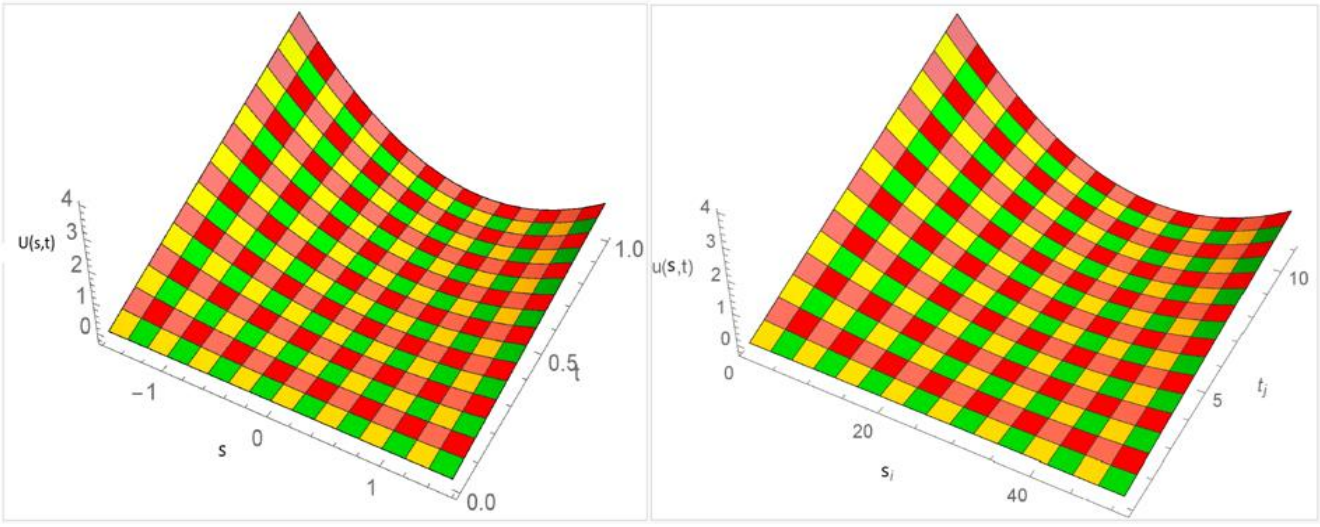

Figure.6 Plot of Exact and Approximate solution for Problem 6.3.

Figure.7 3D plot of Absolute error for Problem 6.3.

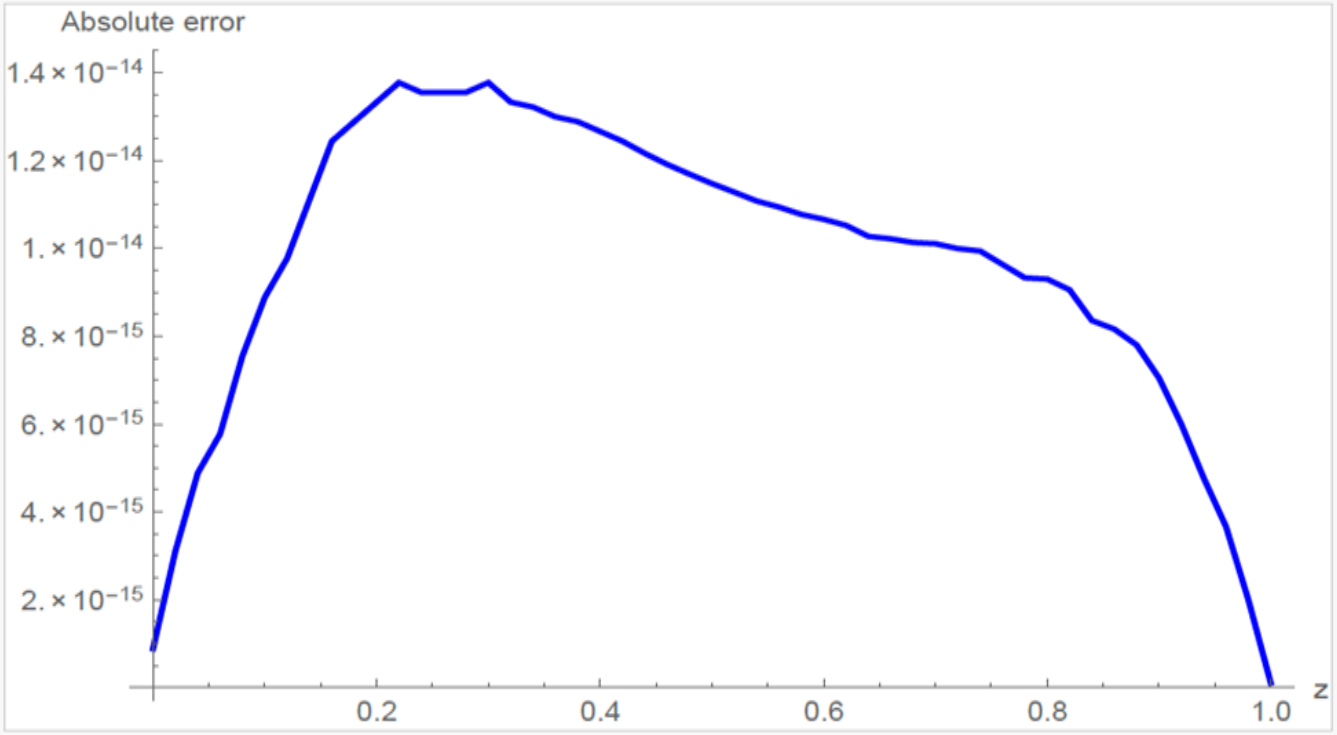

7. Summary and Conclusion

In this work, for solving the multi-term time-fractional telegraph equation, an efficient numerical algorithm has been proposed by utilizing a hybrid B-spline approach. The fractional time derivatives are treated in the Caputo sense, with finite difference formulas used for their discretization, while, the spatial derivatives are approximated using a hybrid B-spline approach. The spatial discretization approach introduced here is shown to be superior to several existing methods, as it provides a continuous and highly accurate approximation of both the solution and its derivatives throughout the domain. The stability of the proposed algorithm has been rigorously established along the temporal grid. Theoretical analysis indicates that the method achieves second-order accuracy in space $O(h2)$ whereas in time direction it is $O(t^{2-\beta})\ when\ \beta = 1+\gamma\ and\ O(t^{1-\beta/2})\ when\ \beta = 2\gamma$. Numerical experiments confirm that the observed convergence rates are consistent with the theoretical predictions. Furthermore, comparisons of error norms demonstrate that the proposed method surpasses previously reported techniques [28, 30, 33, 40] in terms of both accuracy and simplicity of implementation.

Declaration of Competing Interest: The authors confirm that they have no financial or personal affiliations that could have influenced the content or outcomes of this study.

Acknowledgment: The author extends sincere gratitude to Dr. Saima Mushtaq, Superior University Lahore, Pakistan, for her valuable assistance in proofreading the manuscript.

Funding Statement: This research was carried out without any specific grant from funding agencies in the public, commercial, or not-for-profit sectors.

References

Priyanka, Singh, A., Kumar, S., & Vigo-Aguiar, J. (2025). A Fast High-Order Nonpolynomial Spline Method for Nonlinear Time-Fractional Telegraph Model for Neutron Transport in a Nuclear Reactor. Mathematical Methods in the Applied Sciences, 48(9), 9751-9769.

Modanli M, Akgül A. On solutions of fractional order telegraph partial differential equation by Crank-Nicholson finite difference method. Appl Math Nonlinear Sci 2020;5(1):163-70.

Kumar A, Bhardwaj A, Dubey S. A local meshless method to approximate the time-fractional telegraph equation. Eng Comput 2021;37(4):3473-88.

Ibrahim W, Bijiga LK. Neural network method for solving time- fractional telegraph equation. Math Probl Eng 2021;(2021).

Hafez RM, Youssri YH. Shifted Jacobi collocation scheme for multidimensional time-fractional order telegraph equation. Iran J Numer Anal Optim 2020;10(1):195-223.

Mirzaee F, Samadyar N. Implicit meshless method to solve 2D fractional stochastic Tricomi-type equation defined on irregular domain occurring in fractal transonic flow. Numer Methods Partial Differential Equations 2021;37(2):1781-99.

Hassani H, Avazzadeh Z, Machado JA. Numerical approach for solving variable-order space-time fractional telegraph equation using transcendental Bernstein series. Eng Comput 2020;36(3):867-78.

Wang J, Yin B, Liu Y, Li H, Fang Z. Mixed finite element algorithm for a nonlinear time fractional wave model. Math Comput Simulation 2021;188:60-76.

Haq F, Shah K, Shahzad M. Hyers-Ulam stability to a class of fractional differential equations with boundary conditions. Int J Appl Comput Math 2017;3(1):1135-47.

Samadyar N, Mirzaee F. Numerical solution of two-dimensional weakly singular stochastic integral equations on non-rectangular domains via radial basis functions. Eng Anal Bound Elem 2019;101:27-36.

Yaseen M, Abbas M. An efficient cubic trigonometric B-spline collocation scheme for the time-fractional telegraph equation. Appl Math- J Chin Univ 2020;35(3):359-78.

Redhwan SS, Abdo MS, Shah K, Abdeljawad T, Dawood S, Abdo HA, et al. Mathematical modeling for the outbreak of the coronavirus (COVID-19) under fractional nonlocal operator. Results Phys 2020;19:103610.

Shivhare M, Podila PC, Ramos H, Vigo-Aguiar J. Quadratic B-spline collocation method for time dependent singularly perturbed differential-difference equation arising in the modeling of neuronal activity. Numer Methods Partial Differential Equations 2021.

Hafez RM. Numerical solution of linear and nonlinear hyperbolic telegraph type equations with variable coefficients using shifted Jacobi collocation method. Comput Appl Math 2018;37(4):5253-73.

Benson, D. A., Schumer, R., Meerschaert, M. M., Wheatcraft, S. W. (2001). Fractional dispersion, lévy motion, and the made tracer tests. Transport in Porous Media, 42(1–2), 211–240. DOI 10.1023/A:1006733002131.

Khalid, N., Abbas, M., Iqbal, M. K., Baleanu, D. (2019). A numerical algorithm based on modified extended B-spline functions for solving time-fractional diffusion wave equation involving reaction and damping terms. Advances in Difference Equations, 2019(1), 378. DOI 10.1186/s13662-019-2318-7.

Wasim, I., Abbas, M., Amin, M. (2018). Hybrid B-spline collocation method for solving the generalized burgers-fisher and burgers-huxley equations. Mathematical Problems in Engineering, 2018(10), 1–18. DOI 10.1155/2018/6143934.

Akram, T., Abbas, M., Ismail, A. I., Ali, N. H. M., Baleanu, D. (2019). Extended cubic B-splines in the numerical solution of time fractional telegraph equation. Advances in Difference Equations, 2019(1), 365. DOI 10.1186/s13662-019-2296-9.

Asif, N., Hammouch, Z., Riaz, M., Bulut, H. (2018). Analytical solution of a maxwell fluid with slip effects in view of the caputo-fabrizio derivative. European Physical Journal Plus, 133(7), 272. DOI 10.1140/epjp/i2018-12098-6.

Singh, J., Kumar, D., Hammouch, Z., Atangana, A. (2018). A fractional epidemiological model for com-puter viruses pertaining to a new fractional derivative. Applied Mathematics and Computation, 316(30), 504–515. DOI 10.1016/j.amc.2017.08.048.

Weston, V., He, S. (1993). Wave splitting of the telegraph equation in R3 and its application to inverse scattering. Inverse Problems, 9(6), 789–812. DOI 10.1088/0266-5611/9/6/013.

Dehghan, M., Shokri, A. (2008). A numerical method for solving the hyperbolic telegraph equation. Numerical Methods for Partial Differential Equations: An International Journal, 24(4), 1080–1093. DOI 10.1002/num.20306.

El-Azab, M., El-Gamel, M. (2007). A numerical algorithm for the solution of telegraph equations. Applied Mathematics and Computation, 190(1), 757–764. DOI 10.1016/j.amc.2007.01.091.

Momani, S. (2005). Analytic and approximate solutions of the space-and time-fractional telegraph equa-tions. Applied Mathematics and Computation, 170(2), 1126–1134. DOI 10.1016/j.amc.2005.01.009.

Dehghan, M., Yousefi, S., Lotfi, A. (2011). The use of He's variational iteration method for solving the telegraph and fractional telegraph equations. International Journal for Numerical Methods in Biomedical Engineering, 27(2), 219–231. DOI 10.1002/cnm.1293.

Das, S., Vishal, K., Gupta, P., Yildirim, A. (2011). An approximate analytical solution of time-fractional telegraph equation. Applied Mathematics and Computation, 217(18), 7405–7411. DOI 10.1016/j.amc.2011.02.030.

Hayat, U., Mohyud-Din, S. (2013). Homotopy perturbation technique for time fractional telegraph equa-tions. International Journal of Modern Theoretical Physics, 2(1), 33–41. DOI 10.1080/00207160902874653.

Wei, L., Dai, H., Zhang, D., Si, Z. (2014). Fully discrete local discontinuous galerkin method for solving the fractional telegraph equation. Calcolo, 51(1), 175–192. DOI 10.1007/s10092-013-0084-6.

Hosseini, V. R., Chen, W., Avazzadeh, Z. (2014). Numerical solution of fractional telegraph equa-tion by using radial basis functions. Engineering Analysis with Boundary Elements, 38, 31–39. DOI 10.1016/j.enganabound.2013.10.009.

Srivastava, V. K., Awasthi, M. K., Tamsir, M. (2013). Rdtm solution of caputo time fractional-order hyperbolic telegraph equation. AIP Advances, 3(3), 32142. DOI 10.1063/1.4799548.

Wang, J., Zhao, M., Zhang, M., Liu, Y., Li, H. (2014). Numerical analysis of an H1-Galerkin mixed finite element method for time fractional telegraph equation. Scientific World Journal, 2014, 14. DOI 10.1155/2014/371413.

Modanli, M., Akgül, A. (2017). Numerical solution of fractional telegraph differential equa-tions by theta-method. European Physical Journal Special Topics, 226(16–18), 3693–3703. DOI 10.1140/epjst/e2018-00088-6.

Xu, X., Xu, D. (2018). Legendre wavelets direct method for the numerical solution of time-fractional order telegraph equations. Mediterranean Journal of Mathematics, 15(1), 27. DOI 10.1007/s00009-018-1074-3.

Wang, Y., Mei, L. (2017). Generalized finite difference/spectral galerkin approximations for the time-fractional telegraph equation. Advances in Difference Equations, 2017(1), 281. DOI 10.1186/s13662-017-1348-2.

Kamran, Uddin, M., & Ali, A. (2018). On the approximation of time-fractional telegraph equations using localized kernel-based method. Advances in Difference Equations, 2018, 1-14.

Xu, G., Wang, G. Z. (2008). Extended cubic uniform B-spline and α-B-spline. Acta Automatica Sinica, 34(8), 980–984. DOI 10.1016/S1874-1029(08)60047-6.

Mohyud-Din, S. T., Akram, T., Abbas, M., Ismail, A. I., Ali, N. H. (2018). A fully implicit finite difference scheme based on extended cubic B-splines for time fractional advection-diffusion equation. Advances in Difference Equations, 2018(1), 109. DOI 10.1186/s13662-018-1537-7.

Ghalib, M. M., Zafar, A. A., Hammouch, Z., Riaz, M. B., Shabbir, K. (2020). Analytical results on the unsteady rotational flow of fractional-order non-newtonian fluids with shear stress on the boundary. Discrete & Continuous Dynamical Systems-S, 13(3), 683–693. DOI 10.3934/dcdss.2020037.

Uçar, S., Uçar, E., Özdemir, N., Hammouch, Z. (2019). Mathematical analysis and numerical simulation for a smoking model with Atangana–Baleanu derivative. Chaos, Solitons & Fractals, 118, 300–306. DOI 10.1016/j.chaos.2018.12.003

Owolabi, K. M., Hammouch, Z. (2019). Spatiotemporal patterns in the Belousov–Zhabotinskii reac-tion systems with atangana-baleanu fractional order derivative. Physica A: Statistical Mechanics and its Applications, 523(303), 1072–1090. DOI 10.1016/j.physa.2019.04.017.